International Research Journal of Engineering and Technology (IRJET) e-ISSN: 2395-0056
Volume: 08 Issue: 08 | Aug 2021 www.irjet.net p-ISSN: 2395-0072

Research on Coupling between Ground Water Seepage and Freezing Temperature Field and the Mechanism Used for Artificial Frozen Wall

Yunusa Halliru[1], Chuanxin Rong[2], Shichen Sun[3], Abubakar Sadiq Lawi[4]

[1-4]*First School of Civil Engineering and Architecture, Anhui University of Science and Technology, Huainan, China*

Abstract - Aiming at the problem of excessive deformation and even instability of reinforced earth and ground water seepage retaining during the construction of freezing wells. The most common problems are irregular geometry of the frozen wall formed under the condition of leaking water, the development of uneven thickness, which leads to a partial thinning of the thickness of the frozen wall, an increase in the average temperature of the frozen wall, which leads to a partial decrease in the strength and stability of the frozen wall, etc. Therefore, it is necessary to examine the effect of leakage rate on the temperature field of the freezing process through similar simulation tests. For this reason, this article presents the effect of stratospheric water flow rate and freezing tube is melt on the freezing process and analyzes the effect of various factors on the temperature field during freezing according to the test results. In addition, according to the analysis of the distribution characteristics of the frozen temperature field, the difference between the thickness of the frozen wall along the main surface and the upper and lower reach of the interface is also examined.

***Key Words*: Frozen wall, ground water, seepage, soil, temperature**

1. INTRODUCTION

In recent years, the development of buildings has also developed from high-rise buildings to underground, and the demand for deep underground structures from energy development departments has also increased. Therefore, the scale of underground space development has rapidly increased[1]. The requirements of various building codes on the anti-floating design of underground structures are rather vague, and most require a certain reduction ratio to be determined based on engineering experience. In the construction of urban subways, building foundations, subsea tunnels and other projects, the artificial soil freezing method is often used to temporarily strengthen the strength of the soil[2]. The soil layer can greatly increase its strength during the freezing period to meet engineering needs, and it can be restored to its original state after freezing and melting, reducing environmental pollution and damage. In addition, Frozen soil is a porous medium material whose temperature is not higher than 0°C and soil particles are cemented by ice[3]. According to the duration of freezing, it can be divided into seasonal frozen soil and permafrost. With the increasingly serious environmental factors such as global warming, the impact of frozen soil on the environment and engineering has gradually received great attention from scholars and technicians[4]. Frost heave is a phenomenon in which the volume of the soil expands when the water in the soil freezes, resulting in an increase in the volume of the soil. As the most common physical and mechanical phenomenon in frozen soil, frost heave has an important influence on the destruction of landforms[5].

In the elaboration of frozen walls, the configuration temperature and groundwater flow circulation will interrelate together[6]. However, flow of groundwater takes away cooling over the freezing pillars and dawdling the cooling process of the formation and as the temperature of the formation decreases the flow of groundwater will also be affected. When the temperature extends to freezing level, pores change in freezing water, resulting in ice formation. Therefore, this will lead to alterations in material properties of soil[7]. Furthermore, For the weak soil areas such as river network mud areas, the soil can be frozen by directly laying freezing pipes to increase the strength of the soil. In the temporary roads, for areas with high environmental protection requirements, a freezing layer can be erected on the ground and frozen by artificial water injection to form temporary roads on the protected surface[8]. The temporary road formed by the artificial freezing method can be restored to its original state in a short time after the vehicle passes. It can be frozen 1 to 2 days before the next vehicle passes and can be restored to its original state after passing. The construction flexibility and cost are both acceptable[9].

1.1 Literature Review

In literature [10] an author preset a model of the limited element of coupled thermo hydraulic is proposed to optimize ground freezing in the tunnel by finding the optimal position of the frozen tube, considering the leakage flow, by using ACO method to integrate frozen soil in the optimization. In [11] author proposed a method of sealing the water over the tube liner by a disparity control freezing method by means of twofold dins of shack. In [12] outlines work to control the spread pf radionuclides and

to release them to the ocean through hydrological means. As initial reaction, filthy water is stored in a water tank pending action. However, regulated the storage volume and the danger of seepage build measurement unsortable in the long run. Authors represent a combined mathematical model of thermal hydraulics that is thermodynamically identical and is proposed to reproduce artificial ground freezing of saturated and non-deformed porous media under leaching flow circumstance [13]. An author research on the stress distribution characteristics, deformation and failure characteristics of the floor rock mass, and the mechanism of floor water inrush in the mining face and obtained a lot of useful research results [14]. Researcher in [15] considered the water content, temperature, fineness, and compactness, etc. Influencing factors, the indoor frost heave test was designed by the orthogonal test method, and it was found that the water content has the greatest influence on the frost heave. An author [16] studied the movement speed of the freezing front through an indoor unidirectional frost heave test. During the frost heave process, a lower cold end temperature can increase the movement speed of the freezing front; The freezing and migration rate is affected by the combination of external factors (such as the temperature of the cold end of the soil). In [17] concluded that the constraints of water resources on the sustainable development of cities are mainly manifested in functional constraints, ecological constraints, economic constraints, and institutional constraints aspect. To explore the load-bearing characteristics of artificially frozen roadbeds in the construction of power transmission lines, a model test of the mechanical properties of artificially frozen roadbeds was carried out, and the physical and mechanical properties of ice and frozen soil samples were experimentally studied [18]. According to the pipe jacking method, [19] analyzed the method of foundation reinforcement during excavation in the case of poor soil quality and large seepage. An author [20] made observations on the temperature field of roadbeds in cold areas and analyzed the freezing depth and freezing-thawing changes of roadbeds.

2. SYSTEM MODELING

The process of forming frozen walls under the action of seepage water is studied using the two-hole gel model, which includes three physical systems, the freezing temperature field system, the groundwater infiltration field system, and the freezer heat exchange system. The main factors affecting the formation of frozen walls work by affecting all three systems, the main factors of which are as follows[21].

Factors involved in the freezer heat exchanger system: freezer tube diameter D_b(m), flow rate of alcohol V_y(m/s), Alcohol power stickiness coefficient u_b[kg/(ms)], alcohol adhesion factor, u-b. (kg/(ms)), freezer heat exchanger coefficient, h_b [kg/ (s^3 °C)], alcohol density, ρ_v (kg/m^3), thermal conductivity, λ_b (kgm/(s^3°C), heat ratio, Cb [m^2/(s^2°C), alcohol temperature, Ty [°C].

The factors involved in the formation seepage field system are groundwater flow velocity Vn[m/s], hydrodynamic viscosity coefficient u_w[kg/(ms)], seep water pressure Δp[kg/(ms2)], penetration K[m2], hydraulic path ΔL[m] [22].

Factors involved in the two-hole freezing model formation temperature field system: x-axis X[m], y-axis Y[m], any point in the formation P(X,Y), temperature T[°C], freeze tube diameter Db[m], Freeze the tube placement spacing S[m], The original ground temperature of the formation (infinite distance) T_∞[°C], freeze the tube wall temperature T_b[°C], the temperature conductivity of the unfrozen soil in the formation α_{su}[m^2/s], the temperature conductivity coefficient of the formation permafrost α_{sf}[m^2/s], the temperature conductivity of water α_w[m^2/s], freeze time τ[s], or freeze the wall circle time τ_j, alcohol flow Q[m^3/s], groundwater flow rate V_n[m/s], freeze wall thickness E[m], upstream thickness E_u[m], downstream thickness E_d[m], Phase-changed latent heat q[kg/(ms^2)] [23].

Therefore, the function relationship is [24],

$$[f(D_b, V_y, u_b, h_b, \rho_y, \lambda_b, C_b, T_y, V_n, u_w, \Delta p, K, \Delta L, X, Y, T, S, T_\infty, T_b, \alpha_{su}, \alpha_{sf}, \alpha_w, \tau, Q, E, q = 0] \quad (1)$$

Build equations based on the principle of intrinsically harmony.

$$[\pi = D_b^{x_1} V_y^{x_2} u_b^{x_3} h_b^{x_4} \rho_y^{x_5} \lambda_b^{x_6} c_b^{x_7} T_y^{x_8} V_n^{x_9} u_w^{x_{10}} \Delta P^{x11} K^{x_{12}} \Delta L^{x_{13}} X^{x_{14}} Y^{x_{15}} T^{x_{16}} S^{x_{17}} T_\infty^{x_{18}} T_b^{x_{19}} \cdot \alpha_{su}^{x_{20}} \alpha_{sf}^{x_{21}} \alpha_w^{x_{22}} \tau^{x_{23}} Q^{x_{24}} E^{x_{25}} q^{x_{26}}] \quad (2)$$

2.1. Geometric Similarity Ratio

To determine the test geometric indentation mainly considers the actual situation of freezing pipe diameter, freezing tube arrangement spacing, freezing temperature field influence range, seepage field boundary conditions, test conditions, model processing process and other requirements, according to which the design selects the geometric similarity ratio, $C_l = 1/5$ [25].

According to the geometric guidelines, π5, π10, π11, π12, π14 get the geometric indentation of frozen wall thickness E, freeze hole arrangement spacing S, frozen temperature field coordinates P (x,y), iso-geometric indentation 1/5.

2.2. The Similarity Ratio of Formation Temperature

The single-value conditions of the model and prototype are similar, using similar criteria $\pi_{13} = \frac{T}{T_y}$、$\pi_{15} = \frac{T}{T_\infty}$、$\pi_{16} = \frac{T}{T_b}$ and get $C_T = C_{T_y} = C_{T_\infty} = C_{T_b} = 1$. The temperature of the model is the same as the temperature

of the prototype, so the saline temperature, the temperature of the freezing pipe wall, the original temperature of the formation and the temperature of the water are the same as the engineering temperature [26].

2.3. Similarity Ratio of Test Materials

Freezing tube using seamless steel pipe, refrigerant with alcohol, technique use of saline. Given the main factors affecting refrigerants, sticky coefficient, density, flow rate and cross-section radius of the frozen tube are simply to ensure that alcohol carries the same heat as brine under the same conditions [27]. The similarity of the performance of the model material with the wearer is, $C_{\alpha_{su}} = C_{\alpha_{sf}} = C_{\alpha_w} = C_{u_w} = C_{u_b} = C_{\lambda_b} = C_{C_b} = C_K = C_{\rho_y} = 1$.

2.4. Time Ratio

According to similar guidelines $\pi_{17} = \frac{\alpha_{su}\tau}{S^2}$、$\pi_{18} = \frac{\alpha_{sf}\tau}{S^2}$、$\pi_{19} = \frac{\alpha_w\tau}{S^2}$, get a time-like ratio $C_\tau = C_l^2 = \frac{1}{25}$, That is, the test freeze of 57.6 min is equivalent to the project freeze of 1d.

2.5. Similar Ratio of Stratospheric Seepage Parameters

According to similar instructions, $\pi_{20} = \frac{V_n\tau}{S}$ to achieve a simulated formation water flow rate $C_{V_n} = 5$, The velocity of the water flow in the test 5m/s, equivalent to the actual 1m/s, 5m/d in the experiment corresponds to 1m/d in the project. $\pi_{21} = \frac{Q}{S^2 V_n}$, A similar ratio of alcohol flow in the simulated formation is obtained $C_Q = \frac{1}{5}$, The alcohol flow of 1m ^{3}/h in the test was equivalent to the actual 5m^3/h. Furthermore, $\pi_1 = \frac{D_b V_y \rho_y}{u_b}$、$\pi_8 = \frac{\Delta P}{\rho_y V_y^2}$、$\pi_{10} = \frac{\Delta L}{D_b}$, Similar ratio of seepage pressure in the test $C_{\Delta p} = 25$, Similarity of hydraulic paths $C_{\Delta L} = \frac{1}{5}$.

Table -1: Geometric Similar Parameters

Parameters	Operational	Experiments
Freezing tube	Φ108mm×8mm	Φ21.6mm×1.6mm
Freeze tube spacing	1200mm	24mm
Length	11.5m	2300mm
Width	7.5m	1500mm
Hight	4m	800mm

Table -2: Cooling Parameters

Parameters	Mathematical	Experiments (salt water)	Experiment (alcohol)
Freeze the flow of	7~12m^3/h	1.4~2.4m^3/h	3~5.5m^3/h

Table -3: Seepage parameters

Systematic speed parameters	Experimental Speed parameters
3m/d	15m/d(0.625m/h)
5m/d	25m/d(1.042m/h)
7m/d	35m/d(1.458m/h)
9 m/d	45m/d(1.875m/h)

3. RESULTS AND DISCUSSION

3.1. Experimental Steps

(1) Basic experiments, determine the parameters related to the experiment.

(2) The experimental device is debugged to ensure that the different systems can function properly and coordinate with each other.

(3) Turn on the computer and record the sand layer temperature, water temperature, brine temperature and atmospheric temperature at intervals of 28.8 minutes (quite real 0.5d engineering).

(4) In accordance with the procedures for opening the freezer, adjust the number of freezing cylinders and the control of the throttle valve by the liquid ammonia evaporator, so that the salt water tank reaches the design temperature.

(5) Open the water circulation pump, change the length of the inlet coil immersed in the salt water tank to adjust the water temperature to maintain at about 20 degrees C, adjust the water pressure in the tank modified by the water control valve, control the water flow through the sand layer, so that the rate of infiltration water in the sand layer to reach the nominal value, the simulation formation of the infiltration water formation.

(6) When the temperature of the salt water meets the design requirements, turn on the salt water pump, adjust the flow rate and pressure of the salt water to reach the nominal value, form the simulation system of the circulation of salt water, record the opening time of the pump.

(7) According to the sand layer temperature monitoring record, to determine the arrangement upstream of the frozen wall to the design position, stop the salt pump termination test and record the freezing time.

(8) Close the salt water pipe valve, open the water control valve through the frozen pipe, form a clean water cycle in the frozen pipe, restore the soil temperature of the sand layer.

(9) When the temperature of the sand layer reaches the initial temperature of about C, stop freezing the pipe water cycle, repeat the next series of tests.

3.2 Seepage Simulation System

Darcy's law defines the rate of seepage as the amount of water per unit of time passing through the cross-sectional area of the formation, i.e.: $\nu = \frac{Q}{A} = \frac{K' \Delta H}{L}$. If flow control is used to control the flow rate, the precise control of the flow Q is shown in the table below, the appropriate peristaltic pump needs to be selected according to the maximum flow, but no product can be found to reach the maximum flow rate.

Tab. 4 Seepage flow rate

ν (m/d)	15	25	35	45
Q (ml/min)	12500	20800	29166.67	37500
ΔH(MPa)	0.5/K'	1/K'	1.5/K'	5/K'

So there are two scenarios that we can take for the realization of stable flow rates:

Scenario 1: Take flow control: Use the power pump to provide a fixed flow, and through the spherical control valve and PID regulator to get real-time flow control and display.

Scenario 2: Pressure control: the use of power pumps to provide the base pressure, and through the shunt system and pressure monitoring device to control the pressure to meet the constant pressure difference required upstream and downstream. Both sets of programs have their own oscillations, scheme one is not mentioned in the literature at the moment, in the actual operation process there are more uncertainties, but its accuracy can be guaranteed. The second is to apply more methods, but it must determine the coefficient of hydraulic conduction and the accuracy is low. In order to shorten the preparation time of the test, the optimization of accuracy and control is carried out by taking diagram two as a prototype in the test system.

3.3. Temperature measurement system

The temperature inside the model is fully detected by the thermocouple temperature measurement system, which is mainly composed of Kang Copper, a copper thermocouple chain, a zero-point thermostatic bottle, a multipoint terminal box and a TDS data acquisition instrument. The temperature test of this experiment consists of three parts: the measurement of the temperature of the sand layer and the measurement of the temperature of the saline and clean water of the fluids. The measuring point of the temperature of the sand layer is arranged at two main horizontal and auxiliary levels, the temperature measuring point is mainly the main level, the auxiliary level is arranged as the reference point the measuring point of the main horizontal temperature is arranged at the intermediate level of the sand layer, and the auxiliary level is in the sand layer above the main level of 50 mm.

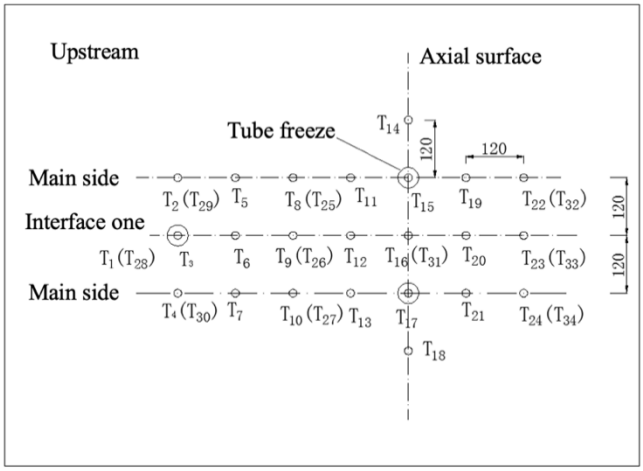

Fig. 1 Temperature measurement

3.4. Experimental Analysis

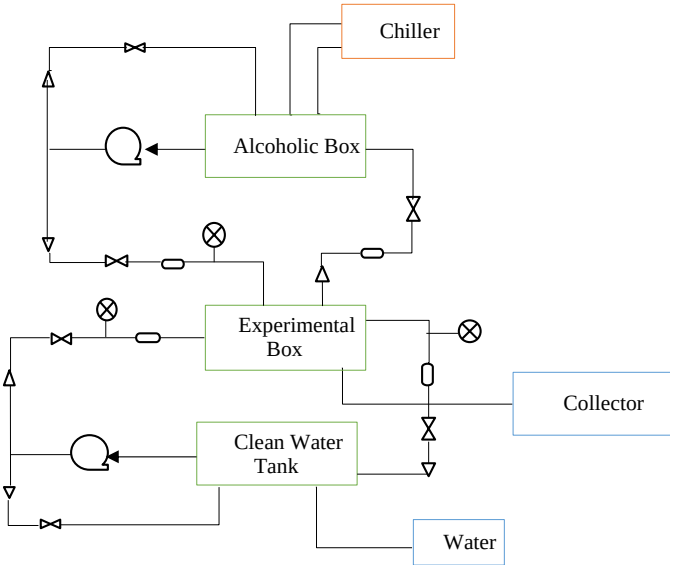

Fig. 2 Structure diagram

Based on the engineering design structure diagram of the entire system is shown in Fig. 2, it can be seen from the Fig. 1, structure diagram mainly consists of chiller, alcoholic box, experimental box, collector, and clean water tank. However, the experimental diagram structure is shown in Fig. 3. Physical structure diagram of the experimental tank is shown in Fig. 4 and constant pressure variable frequency pump diagram is shown in Fig. 5.

The experimental tank is divided into three parts: 300mm in the shower room, 2300mm in the lower test room and

200mm in the shower room, with a total length of 2800mm, a width of 1500mm and a height of 800mm. Each installation of 8 specifications for the 40mm×2mm shower room in and out of the water pipe. Fill the bathroom with stones to dampen the flow of water. The box is made of metal steel plate Q235A with thickness of 15 mm, according to the design working pressure test requirements of the box 0.3Mpa, the other parts are welding, welding rod for J422.

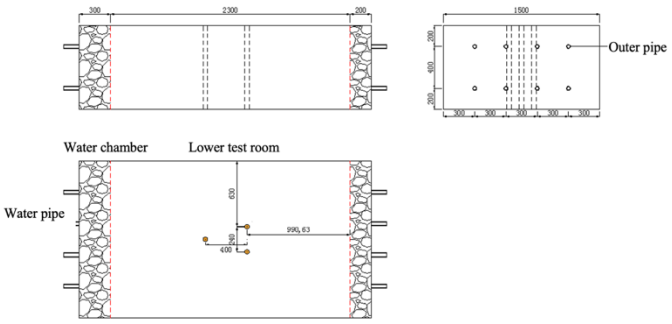

Fig. 3 Experimental diagram

Fig. 4 Physical structure of the experimental tank

Fig. 4 Constant pressure variable frequency pump

The maximum flow rate of the constant pressure pump can reach 8m3/h, which can be controlled by controlling the output pressure of the pump and the sensitive spherical valve, combined with the flow meter reading. If flow control is used to control the flow rate, the precise control of the flow Q is shown in the table below, the appropriate peristaltic pump needs to be selected according to the maximum flow, but no product can be found to reach the maximum flow rate. Variable frequency regulator pumps can be used to provide stable flow and simultaneously monitor pressure, and the electromagnetic flow meter for real-time flow control and display.

4. CONCLUSION

Based on the continuous formation mechanism of the frozen wall and coupling between ground water seepage and freezing temperature, a new coupling model is designed. The change of frozen wall caused by leaking water is reflected in the frozen structure as a control formation, necessary design parameters are adjusted accordingly, such as the arrangement of the freezer holes, the distance of the wheels and wheels, the freezing time, the cooling capacity of the freezer station, etc. In addition, a temperature measurement system is designed, and according to the analysis of the distribution characteristics of the frozen temperature field, the difference between the time of penetration of the frozen wall along the main surface and the upstream and downstream interface is examined.

REFERENCES

[1] M. Chai, J. Zhang, H. Zhang, Y. Mu, G. Sun, and Z. Yin, 'A method for calculating unfrozen water content of silty clay with consideration of freezing point', Appl. Clay Sci., vol. 161, pp. 474–481, Sep. 2018, doi: 10.1016/j.clay.2018.05.015.

[2] K. Xue, Z. Wen, Z. Zhu, D. Wang, F. Luo, and M. Zhang, 'An experimental study of the relationship between the matric potential, unfrozen water, and segregated ice of saturated freezing soil', Bull. Eng. Geol. Environ., vol. 80, no. 3, pp. 2535–2544, Mar. 2021, doi: 10.1007/s10064-020-02052-x.

[3] G. P. Newman and D. Maishman, 'Artificial ground freezing of the McArthur River uranium ore deposit', in Ground Freezing 2000 - Frost Action in Soils, 1st ed., J.-F. Thimus, Ed. CRC Press, 2020, pp. 317–321. doi: 10.1201/9781003078654-63.

[4] A. Marwan, M.-M. Zhou, M. Zaki Abdelrehim, and G. Meschke, 'Optimization of artificial ground freezing in tunneling in the presence of seepage flow', Comput. Geotech., vol. 75, pp. 112–125, May 2016, doi: 10.1016/j.compgeo.2016.01.004.

[5] Y. Liu, K. Li, P. Li, and J. Hu, 'Artificial Ground Freezing Technique in Tunnel Construction Considering Uncertain Drilling Inaccuracy of Freeze Pipes', in Proceedings of the 29th European Safety and Reliability Conference (ESREL), 2019, pp. 3138–3143. doi: 10.3850/978-981-11-2724-3_1063-cd.

[6] Z. Li, J. Chen, M. Sugimoto, and H. Ge, 'Numerical simulation model of artificial ground freezing for tunneling under seepage flow conditions', Tunn.

Undergr. Space Technol., vol. 92, p. 103035, Oct. 2019, doi: 10.1016/j.tust.2019.103035.

[7] M. A. Alzoubi, M. Xu, F. P. Hassani, S. Poncet, and A. P. Sasmito, 'Artificial ground freezing: A review of thermal and hydraulic aspects', Tunn. Undergr. Space Technol., vol. 104, p. 103534, Oct. 2020, doi: 10.1016/j.tust.2020.103534.

[8] R. Hu, Q. Liu, and Y. Xing, 'Case Study of Heat Transfer during Artificial Ground Freezing with Groundwater Flow', Water, vol. 10, no. 10, p. 1322, Sep. 2018, doi: 10.3390/w10101322.

[9] M. A. Alzoubi, A. Nie-Rouquette, and A. P. Sasmito, 'Conjugate heat transfer in artificial ground freezing using enthalpy-porosity method: Experiments and model validation', Int. J. Heat Mass Transf., vol. 126, pp. 740–752, Nov. 2018, doi: 10.1016/j.ijheatmasstransfer.2018.05.059.

[10] Y. Liu, K.-Q. Li, D.-Q. Li, X.-S. Tang, and S.-X. Gu, 'Coupled thermal–hydraulic modeling of artificial ground freezing with uncertainties in pipe inclination and thermal conductivity', Acta Geotech., May 2021, doi: 10.1007/s11440-021-01221-w.

[11] S. Suzuki, 'Dependence of unfrozen water content in unsaturated frozen clay soil on initial soil moisture content', Soil Sci. Plant Nutr., vol. 50, no. 4, pp. 603–606, Feb. 2004, doi: 10.1080/00380768.2004.10408518.

[12] A. O. Sinitsyn and S. Loset, 'Equivalent cohesion of frozen saline sandy loams at temperatures close to their freezing point', Soil Mech. Found. Eng., vol. 47, no. 2, pp. 68–73, Jul. 2010, doi: 10.1007/s11204-010-9091-7.

[13] Z. Wen et al., 'Experimental study on unfrozen water content and soil matric potential of Qinghai-Tibetan silty clay', Environ. Earth Sci., vol. 66, no. 5, pp. 1467–1476, Jul. 2012, doi: 10.1007/s12665-011-1386-0.

[14] W. Fan and P. Yang, 'Ground temperature characteristics during artificial freezing around a subway cross passage', Transp. Geotech., vol. 20, p. 100250, Sep. 2019, doi: 10.1016/j.trgeo.2019.100250.

[15] K. A. Fikiin, 'Generalized numerical modelling of unsteady heat transfer during cooling and freezing using an improved enthalpy method and quasi-one-dimensional formulation', Int. J. Refrig., vol. 19, no. 2, pp. 132–140, Jan. 1996, doi: 10.1016/0140-7007(95)00055-0.

[16] M. A. Alzoubi, A. Madiseh, F. P. Hassani, and A. P. Sasmito, 'Heat transfer analysis in artificial ground freezing under high seepage: Validation and heatlines visualization', Int. J. Therm. Sci., vol. 139, pp. 232–245, May 2019, doi: 10.1016/j.ijthermalsci.2019.02.005.

[17] R. A. Sudisman, M. Osada, and T. Yamabe, 'Heat Transfer Visualization of the Application of a Cooling Pipe in Sand with Flowing Pore Water', J. Cold Reg. Eng., vol. 31, no. 1, p. 04016007, Mar. 2017, doi: 10.1061/(ASCE)CR.1943-5495.0000115.

[18] F. Ming, L. Chen, D. Li, and C. Du, 'Investigation into Freezing Point Depression in Soil Caused by NaCl Solution', Water, vol. 12, no. 8, p. 2232, Aug. 2020, doi: 10.3390/w12082232.

[19] H. Bing and W. Ma, 'Laboratory investigation of the freezing point of saline soil', Cold Reg. Sci. Technol., vol. 67, no. 1–2, pp. 79–88, Jun. 2011, doi: 10.1016/j.coldregions.2011.02.008.

[20] E. Pimentel, A. Sres, and G. Anagnostou, 'Large-scale laboratory tests on artificial ground freezing under seepage-flow conditions', Géotechnique, vol. 62, no. 3, pp. 227–241, Mar. 2012, doi: 10.1680/geot.9.P.120.

[21] P. Qiu, P. Li, J. Hu, and Y. Liu, 'Modeling Seepage Flow and Spatial Variability of Soil Thermal Conductivity during Artificial Ground Freezing for Tunnel Excavation', Appl. Sci., vol. 11, no. 14, p. 6275, Jul. 2021, doi: 10.3390/app11146275.

[22] S. Springman, J. Laue, and L. Seward, Eds., 'Large-scale physical model for simulation of artificial ground freezing with seepage flow', in Physical Modelling in Geotechnics, Two Volume Set, 0 ed., CRC Press, 2010, pp. 405–408. doi: 10.1201/b10554-63.

[23] P. E. Frivik and G. Comini, 'Seepage and Heat Flow in Soil Freezing', J. Heat Transf., vol. 104, no. 2, pp. 323–328, May 1982, doi: 10.1115/1.3245091.

[24] J. A. Sopko, G. F. Aluce, and M. Vliegenthart, 'Methods used in the excavation of shafts supported by artificial ground freezing', in North American Tunneling 2002, 1st ed., L. Ozdemir, Ed. CRC Press, 2021, pp. 263–268. doi: 10.1201/9781003211341-39.

[25] M. Vitel, A. Rouabhi, M. Tijani, and F. Guérin, 'Modeling heat and mass transfer during ground freezing subjected to high seepage velocities', Comput. Geotech., vol. 73, pp. 1–15, Mar. 2016, doi: 10.1016/j.compgeo.2015.11.014.

[26] N. Massarotti, A. Mauro, and V. Trombetta, 'Sparce Subspace Learning and Characteristic Based Split for Modelling Artificial Ground Freezing', Int. J. Heat Mass Transf., vol. 180, p. 121789, Dec. 2021, doi: 10.1016/j.ijheatmasstransfer.2021.121789.

[27] S. Huang, Y. Guo, Y. Liu, L. Ke, G. Liu, and C. chen, 'Study on the influence of water flow on temperature around freeze pipes and its distribution optimization during artificial ground freezing', Appl. Therm. Eng., vol. 135, pp. 435–445, May 2018, doi: 10.1016/j.applthermaleng.2018.02.090.